Metastable states during dissociation of carbon dioxide hydrates below 273 K

V.P. Melnikov [a,b], A.N. Nesterov [a,b,*], A.M. Reshetnikov [a], V.A. Istomin [c]

[a] *Institute of Earth Cryosphere, SB RAS, P.O. 1230, 625000 Tyumen, Russian Federation*
[b] *Tyumen State Oil and Gas University, ul. Volodarskogo 38, 625000 Tyumen, Russian Federation*
[c] *Research Institute of Natural Gases and Gas Technologies (Gazprom VNIIGAZ JSC), 142717 Razvilka, Moskovskaja Oblast, Russian Federation*

ABSTRACT

In this study, the dissociation of isolated carbon dioxide hydrate particles of sizes in the range 0.25–2.5 mm was investigated. It was found that below the ice melting point, the hydrates dissociated into supercooled water (metastable liquid) and gas. The formation of the liquid phase during CO_2 hydrate dissociation was visually observed, and the pressures of the hydrate dissociation into supercooled water and gas were measured in the temperature range 249–273 K. These pressures agreed well with the calculated data for the supercooled water–hydrate–gas metastable equilibrium (Istomin et al., 2006). In the *P–T* area on the phase diagram bounded by the ice–hydrate–gas equilibrium curve and the supercooled water–hydrate–gas metastable equilibrium curve, hydrates could exist for a long time because the metastable phase and their stability are not connected to the self-preservation effect. The growth of the metastable CO_2 hydrate film on the surface of supercooled water droplets formed during the hydrate dissociation was observed at pressure above the three-phase supercooled water–hydrate–gas metastable equilibrium pressure but still below the three-phase ice–hydrate–gas equilibrium pressure. It was found that the growth rate of the metastable CO_2 hydrate film was higher by a factor of 25 and 50 than that for methane hydrate and propane hydrate, respectively.

© 2010 Elsevier Ltd. All rights reserved.

1. Introduction

The unexpected stability of clathrate hydrates of some gases at temperatures below the ice melting point outside their stable region, known as the self-preservation effect (Yakushev and Istomin, 1992) or the anomalous preservation regime (Stern et al., 2001), has also been observed for CO_2 hydrates (Chuvilin et al., 2007; Circone et al., 2003; Falenty and Kuhs, 2009; Kuhs et al., 2004; Takeya and Ripmeester, 2008). The particular interest in the stability and dissociation of CO_2 hydrates below 273 K is due the development of a conceptual idea for CO_2 sequestration as a hydrate in permafrost to reduce the emission of carbon dioxide into the atmosphere and abate global warming (Duchkov et al., 2009; Goel, 2006).

Because the anomalous stability of hydrates outside their stable region was observed only below the ice melting point, it was proposed that the effect was caused by the formation of an ice coating on the surface of hydrate particles (Davidson et al., 1986; Yakushev and Istomin, 1992). Recently, we detected (Melnikov et al., 2010) the existence of metastable methane and propane hydrates below the three-phase ice–hydrate–gas equilibrium pressure, and the stability of the hydrates was not related with ice

formation on their surface. In the pressure–temperature area between the ice–hydrate–gas equilibrium curve and the supercooled water–hydrate–gas metastable equilibrium curve (Fig. 1) hydrate particles that were 0.15–2.5 mm in diameter existed for a prolonged time without visually observed evidence of hydrate dissociation. The hydrates were dissociated into supercooled water and gas when crossing the supercooled water–hydrate–gas metastable equilibrium curve once the pressure was decreased or the temperature was increased. The formation of supercooled water on dissociation of methane hydrate was detected in the range 253–273 K (Melnikov et al., 2009) and 257–273 K on dissociation of propane hydrate (Mel'nikov et al., 2007).

In this communication, the results of a study on behavior of CO_2 hydrate particles outside the hydrate stable region below the ice melting point are presented.

2. Experimental section

CO_2 gas (99.9 mol%) and distilled water were used to synthesize hydrate samples. A detailed description of the experimental setup used in this work and the hydrate synthesis procedure are given elsewhere (Melnikov et al., 2009; Mel'nikov et al., 2007). The main element of the experimental setup was a stainless steel cylindrical reactor with a volume of 100 ccm. For visual observation, the lateral surface of the reactor was equipped with two quartz windows

* Corresponding author at: Institute of Earth Cryosphere, SB RAS, P.O. 1230, 625000 Tyumen, Russian Federation. Tel.: +7 3452 68 87 22; fax: +7 3452 68 87 87.
E-mail addresses: nesterov@ikz.ru, anikz@rambler.ru (A.N. Nesterov).
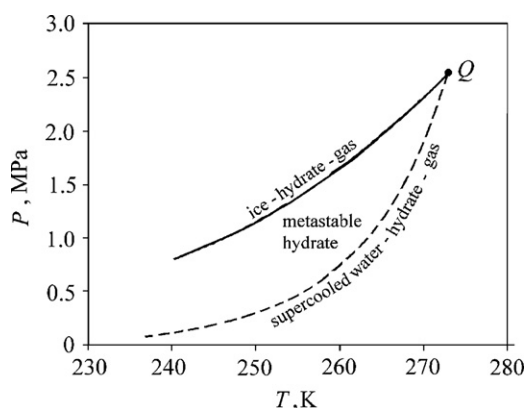
Fig. 1. Phase diagram for the H_2O–CH_4 system. Solid line is the ice–hydrate–gas equilibrium curve and dashed line is the supercooled water–hydrate–gas metastable equilibrium curve. Q is the quadruple point, where ice+water+hydrate+gas coexist (modified from Melnikov et al. (2010)).

located opposite to one another at the half-height of the reactor. Hydrates were formed from water sprayed on a transparent Plexiglas plate. The plate was previously cooled to 253–255 K to form frozen droplets of 0.25–2.5 mm diameter and about 0.3 mm thickness. The plate with frozen droplets was mounted vertically inside the reactor between the windows. The pressure in the reactor was measured by a transducer with an accuracy of 0.01 MPa. Two copper–constantan thermocouples were used to measure the temperature inside the reactor at the top and bottom, and the average temperature was calculated. The temperature inside the reactor was maintained with an accuracy of $\pm$ 0.1 K. The reactor with frozen water droplets was evacuated at 255 K and charged with CO_2 gas to a pressure between the equilibrium pressure of CO_2 hydrate and the dew point of carbon dioxide at given temperature.

To increase the rate of hydrate formation, the reactor with gas and water droplets was slowly heated from 255 to 274 K. The melting/freezing procedure (heating of the reactor to 274 K and subsequent cooling to 255 K) was repeated a few times to provide additional conversion of water into hydrates. The same procedure was used by us before synthesizing methane and propane hydrates from frozen water droplets (Melnikov et al., 2009; Mel'nikov et al., 2007).

For optical observation, a cathetometer was used. The cathetometer telescope was fitted with a digital camera, and the picture was recorded in DVD in real time.

To observe the dissociation of hydrates, the pressure in the reactor was slowly reduced at given temperature. The dissociation of the hydrates was judged from the visually observed collapse of the rough surface of the hydrates, the appearance of smooth islands of the liquid phase on hydrate particles, and the evolution of gas bubbles from the liquid. The pressure at which the first changes in hydrate particles were visually observed was taken as the hydrate dissociation pressure P_d at given temperature. After the onset of hydrate dissociation, the subsequent observations were carried out at constant pressure P_d. It should be noted that the influence of hydrate particle size on dissociation pressure P_d was not detected. All the particles were dissociated at the same pressure P_d.

3. Results and discussion

3.1. Supercooled water–CO_2 hydrates–gas metastable equilibrium

The experimental data on CO_2 hydrate dissociation pressure P_d obtained in this study are summarized in Table 1 and plotted in Fig. 2.

Above the quadruple point temperature, P_d is in good agreement with CO_2 hydrate equilibrium pressure calculated by CSMGem program (Sloan and Koh, 2007).

Table 1
Experimental dissociation pressure P_d for CO_2 hydrates formed from water droplets.

T (K)	P (MPa)
$T > 273$ K	
280.2	2.95
279.1	2.49
278.1	2.15
276.0	1.67
274.1	1.34
273.3	1.25
$T < 273$ K	
272.2	1.09
271.2	0.98
270.0	0.85
269.0	0.74
268.1	0.69
267.0	0.60
266.4	0.56
265.2	0.48
264.0	0.43
262.8	0.36
262.0	0.34
260.9	0.29
259.9	0.27
258.9	0.24
258.0	0.21
257.3	0.19
256.2	0.17
254.3	0.14
253.4	0.13
252.0	0.11
250.8	0.09
249.1	0.08
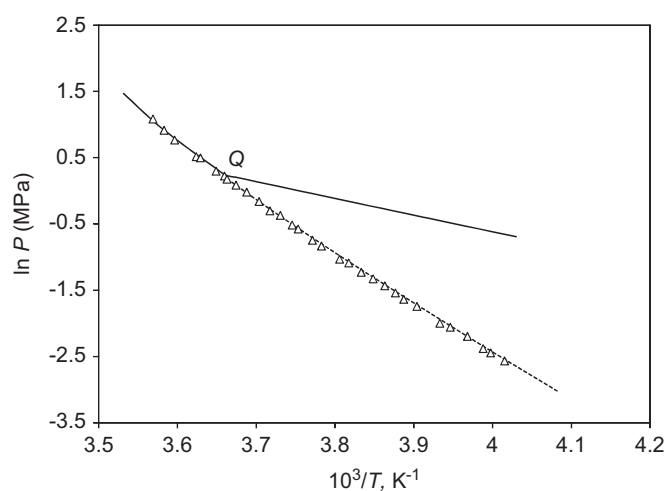
Fig. 2. Dissociation pressure of CO_2 hydrates formed from water droplets (symbols) and the equilibrium pressure of hydrate formation for bulk CO_2 hydrates (—) calculated by the CSMGem program (Sloan and Koh, 2007). Dashed line is the calculated extension of the water–hydrate–methane gas equilibrium curve to the metastable area of supercooled water (Istomin et al., 2006).

Below the quadruple point temperature, the P_d values fall on the supercooled water–CO_2 hydrate–gas metastable equilibrium curve calculated by Istomin et al. (2006). These can be expressed in the form of regression equations as follows:

$$\ln(P_d/P_0) = 28.61 - 7774.7/T, \quad r^2 = 0.9982$$

$$73\,\text{K} < T < 249\,\text{K} \tag{1}$$

where $P_0 = 1$ MPa and r^2 is the regression coefficient.

Fig. 3 shows the successive shots of changes observed visually during the dissociation of CO_2 hydrates at 266.4 K. The first changes in hydrate particles appeared at 0.56 MPa (Fig. 3b). Ice is the stable phase at these conditions, but we observed that the hydrates dissociated into supercooled (metastable) water and gas. The supercooled water lifetime in the metastable state from the beginning of hydrate dissociation until crystallization of supercooled water depended on hydrate dissociation temperature. At 270 K, this stage lasted for tens of hours, but it was a few seconds at 250 K. The absence of ice in the hydrate samples is a necessary constraint to detect supercooled water during hydrate dissociation. Supercooled water cannot coexist with ice, and it freezes instantaneously in the presence of ice. We used isolated small water droplets to synthesize the hydrate samples free from ice. Even though some of hydrate particles formed will contain the ice, they will not influence the behavior of other hydrate particles during their dissociation. It is very difficult to achieve full conversion of water into gas hydrate for bulk samples, even if powdered ice is used. We suppose that presence of ice in hydrate samples can explain that Falenty and Kuhs (2009) in their neutron diffraction experiments had no evidence for any substantial amount of water in the liquid state during the dissociation of bulk hydrate below the ice melting point.

We observed the formation of supercooled water during CO_2 hydrate dissociation up to 249 K. Below this temperature and below the CO_2 hydrate equilibrium pressure no visual changes in the hydrate samples were observed. If the hydrate samples, cooled below 249 K, were heated at a pressure below the hydrate equilibrium pressure, liquid water was observed only near the ice melting point.

3.2. Stability of CO_2 hydrates below the three-phase ice–hydrate–gas equilibrium pressure

We observed the existence of CO_2 hydrates for a long time without visible evidence of the hydrate dissociation in the area bounded by the ice–hydrate–gas equilibrium curve and the supercooled water–hydrate–gas metastable equilibrium curve. Fig. 4 shows the stable CO_2 hydrates (Fig. 4a) and the hydrates, which were stored for 90 h at 264 K and 0.6 MPa (Fig. 4b). The

CO_2 hydrate equilibrium pressure at 264 K is 0.78 MPa, but no visual evidence of hydrate dissociation was detected at 264 K and 0.6 MPa during the entire duration of hydrate observation (90 h). When the pressure in the reactor was decreased, we observed the appearance of supercooled water immediately following the intersection of the supercooled water–hydrate–gas metastable equilibrium curve (Fig. 4c). Based on this, we can conclude that the CO_2 hydrate samples did not contain ice, and the hydrate stability in the area bounded by the ice–hydrate–gas equilibrium curve and the curve of the supercooled water–hydrate–gas metastable equilibrium was not connected with the self-preservation effect. The hydrate observed in our experiments in the area bounded by the ice–hydrate–gas equilibrium curve and the curve of the supercooled water–hydrate–gas metastable equilibrium is an example of the metastable phase, the stability of which is caused by the kinetic difficulty in the direct transformation of the hydrate crystal structure into ice. The stability of the self-preserved hydrate is caused by the slow rate of gas diffusion through the ice layer on the surface of hydrate particles (Takeya et al., 2001).

3.3. Hydrate growth below the three-phase ice–hydrate–gas equilibrium pressure

Fig. 5 shows the lateral growth of the film of metastable CO_2 hydrates at the surface of a supercooled water droplet at 265.2 K and 0.57 MPa. Because of the stochastic nature of hydrate nucleation, hydrates are not formed at the same time on the droplets of supercooled water. In this experiment, after the completion of the hydrate dissociation into supercooled water and gas (hydrates were no longer detected in the water droplets, Fig. 5b), the pressure $P_d=0.48$ MPa was kept in the reactor for the next 10 min and then it was increased to 0.56 MPa, but it still remained below the ice–hydrate–gas equilibrium pressure at 265.2 K, 0.82 MPa. About 1 min after the pressure was increased, the onset of growth of the solid film on the surface of the supercooled water droplet was observed (Fig. 5c). We checked that the solid film in Fig. 5c–f was hydrate by observing that it melted if the pressure was again lowered below P_d.
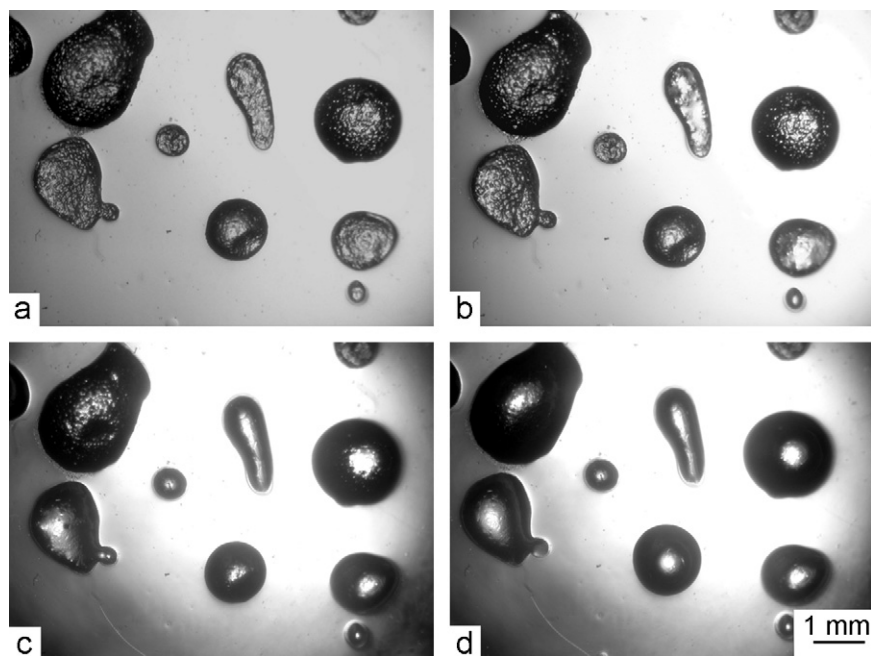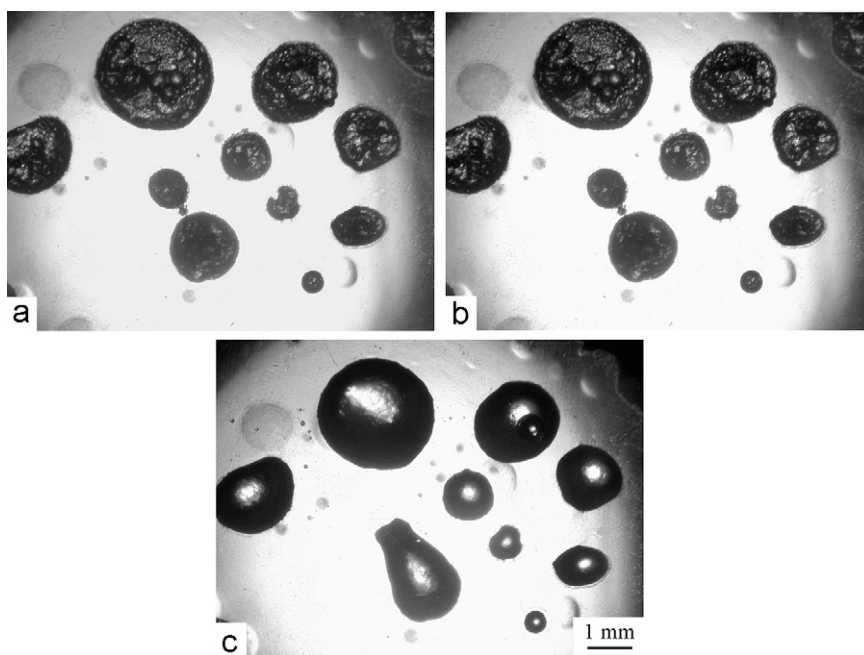

Fig. 3. Formation of supercooled water during CO_2 hydrate dissociation at 266.4 K. (a) At 1.8 MPa (before pressure decrease); (b) onset of hydrate dissociation at 0.56 MPa, time=0; (c) at 0.56 MPa, time=4 min; and (d) at 0.56 MPa, time=14 min.

Fig. 4. (a) Stable CO_2 hydrates at 2 MPa and 264 K; (b) metastable CO_2 hydrates 90 h after the pressure was decreased to 0.6 MPa at 264 K (the CO_2 hydrate equilibrium pressure is 0.78 MPa); and (c) dissociation of CO_2 hydrates into supercooled water and gas at 264 K and 0.43 MPa.
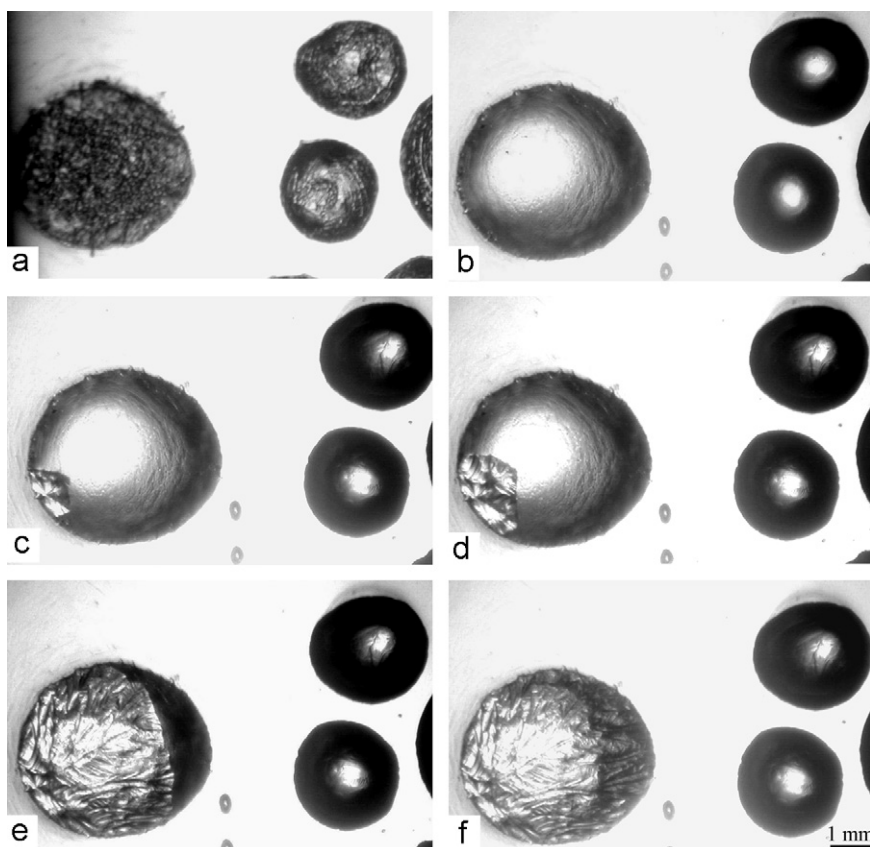
Fig. 5. (a and b) Dissociation of CO_2 hydrates into supercooled water and gas and (c–f) growth of metastable hydrates on the surface of supercooled water at 265.2 K. (a) Onset of hydrate dissociation at 0.48 MPa; (b) 15 min after the onset of hydrate dissociation, $P=0.48$ MPa. Hydrates are no longer detected in the water droplets (the completion of the hydrate dissociation); (c–f) growth of metastable hydrates at 0.56 MPa. The pressure of the ice–hydrate–gas equilibrium at 265.2 K is 0.82 MPa.

With the use of video, the lateral growth rates of the CO_2 hydrate film on the surface of supercooled water droplets were measured. The procedure used was described in detail by Freer et al. (2001).

The lateral growth rates of the CO_2 hydrate film on the surface of supercooled water droplets as a function of supercooling ΔT at different system temperatures are shown in Fig. 6. In these
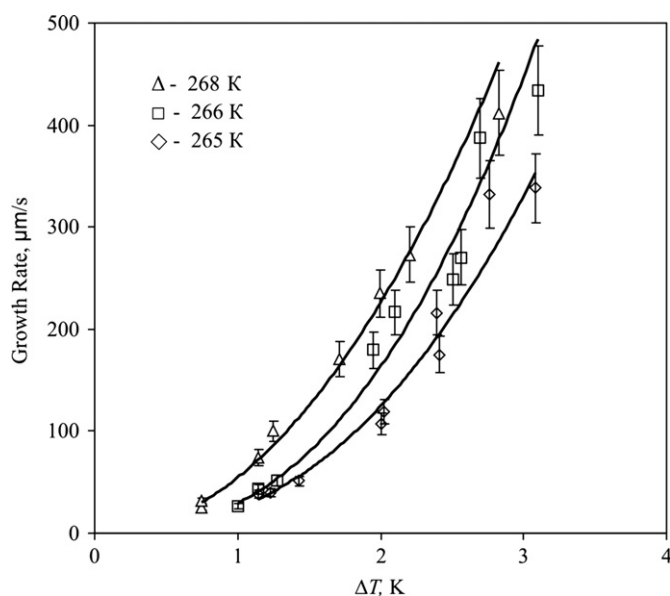
Fig. 6. Lateral growth rate of the film of metastable CO_2 hydrate on the surface of supercooled water droplets formed during the hydrate dissociation.

experiments, water with a previous hydrate history (water obtained by melting CO_2 hydrate at a pressure slightly below the supercooled water–hydrate–gas metastable equilibrium pressure) is used. Here $\Delta T = T_{meq} - T$, where T_{meq} is the temperature of the supercooled water–hydrate–gas metastable equilibrium at the system pressure P, and T is the system temperature. The comparison of the growth rate of the CO_2 hydrate film on the surface of supercooled water droplets with the data on film growth for metastable methane and propane hydrates (Melnikov et al., 2010) demonstrates that the film growth rate for CO_2 hydrate is about 25 times higher than that for methane hydrate and is about 50 times higher than that for propane hydrate. This difference is probably due to the higher solubility of CO_2 gas into water in comparison with the solubility of methane and propane.

4. Conclusions

The formation of liquid supercooled water as a transition state between CO_2 hydrates and ice was visually observed during CO_2 hydrate dissociation between 273 and 249 K. The pressure of the supercooled water–hydrate–gas metastable equilibrium was measured at different temperatures. Evidence for the existence of the metastable CO_2 hydrates was obtained, and the stability of the hydrates was not connected with the ice formation on the hydrate surface in the area bounded by the ice–hydrate–gas equilibrium curve and the supercooled water–hydrate–gas metastable equilibrium curve. The lateral growth rates of the metastable CO_2 hydrate film

on the surface of supercooled water were measured. It was found that the CO_2 hydrate film growth rate was higher by a factor of 25 and 50 than those for methane hydrate and propane hydrate, respectively.

References

Chuvilin, E.M., Petrakova, S.Y., Gureva, O.M., Istomin, V.A., 2007. Formation of carbon dioxide gas hydrates in freezing sediments and decomposition kinetics of the hydrates formed. In: Kuhs, W.F. (Ed.), Physics and Chemistry of Ice. The Royal Society of Chemistry, Cambridge, pp. 147–154.
Circone, S., Stern, L.A., Kirby, S.H., Durham, W.B., Chakoumakos, B., Rawn, C., Rondinone, A., Ishii, Y., 2003. CO_2 hydrate: synthesis, composition, structure, dissociation behavior, and comparison to structure I CH_4 hydrate. Journal of Physical Chemistry B 107, 5529–5539.
Davidson, D.W., Garg, S.K., Gough, S.R., Handa, Y.P., Ratclife, C.I., Ripmeester, J.A., Tse, J.S., Lawson, W.F., 1986. Laboratory analysis of naturally occurring gas hydrate from sediment of the Gulf Mexico. Geochimica et Cosmochimica Acta 50, 619–623.
Duchkov, A.D., Sokolova, L.S., Ayunov, D.E., Permyakov, M.E., 2009. Assesment of potential of Western Siberia permafrost for the carbon dioxide storage. Earth's Cryosphere 13 (4), 62–68 in Russian.
Falenty, A., Kuhs, W.F., 2009. "Self-preservation" of CO_2 gas hydrates—surface microstructure and ice perfection. Journal of Physical Chemistry B 113, 15975–15988.
Freer, E.M., Selim, M.S., Sloan, E.D., 2001. Methane hydrate film growth kinetics. Fluid Phase Equilibria 185, 65–75.
Goel, N., 2006. In situ methane hydrate dissociation with carbon dioxide sequestration: current knowledge and issues. Journal of Petroleum Science and Engineering 51, 169–184.
Istomin, V.A., Kwon, V.G., Durov, V.A., 2006. Metastable states of gas hydrates. Gazovaya Promishlennost (Gas Industry of Russia, Special Issue: Gas Hydrates), 32–35 (in Russian).
Kuhs, W.F., Genov, G., Staykova, D.K., Hansen, T., 2004. Ice perfection and onset of anomalous preservation of gas hydrate. Physical Chemistry Chemical Physics 6, 4917–4920.
Melnikov, V.P., Nesterov, A.N., Reshetnikov, Istomin, V.A., Kwon, V.G., 2010. Stability and growth of gas hydrates below the ice–hydrate–gas equilibrium line on the P–T phase diagram. Chemical Engineering Science 65, 906–914.
Melnikov, V.P., Nesterov, A.N., Reshetnikov, A.M., Zavodovsky, A.G., 2009. Evidence of liquid water formation during methane hydrates dissociation below the ice point. Chemical Engineering Science 64, 1160–1166.
Mel'nikov, V.P., Nesterov, A.N., Reshetnikov, A.M., 2007. Formation of supercooled water upon dissociation of propane hydrates at $T < 270$ K. Doklady Physical Chemistry 417, 304–307.
Sloan, E.D., Koh, C.A., 2007. Clathrate hydrates of natural gases. third ed. CRS Press Taylor and Francis Group, Boca Raton.
Stern, L.A., Circone, S., Kirby, S.H., Durham, W.B., 2001. Anomalous preservation of pure methane hydrate at 1 atm. Journal of Physical Chemistry B 105, 1756–1762.
Takeya, S., Ripmeester, J., 2008. Dissociation behavior of clathrate hydrates to ice and dependence on guest molecules. Angewandte Chemie International Edition 47, 1276–1279.
Takeya, S., Shimada, W., Kamata, Y., Ebinuma, T., Uchida, T., Nagao, J., Narita, H., 2001. In situ X-ray diffraction measurements of the self-preservation effect of CH_4 hydrate. Journal of Physical Chemistry A 105, 9756–9759.
Yakushev, V.S., Istomin, V.A., 1992. Gas hydrate self-preservation effect. In: Maeno, N., Hondoh, T. (Eds.), Physics and Chemistry of Ice.. Hokkaido University Press, Sapporo, pp. 136–140.